

TOPICAL REVIEW

Microfluid mechanics: progress and opportunities

N Giordano and J-T Cheng

Department of Physics, Purdue University, West Lafayette, IN 47907-1396, USA

Received 30 January 2001

Abstract

The application of microfabrication techniques to problems involving fluids is reviewed. A number of scientific issues have been addressed using microstructures designed to confine and manipulate fluids. These problems include studies of fluid motion in percolative structures, chemical applications involving small volumes of reactants and products, biologically inspired experiments involving the manipulation of individual molecules, and studies of fundamental properties of liquids in extremely small geometries. Representative work is described, along with the ingenious fabrication methods which have been developed.

We believe that there are many opportunities for interesting basic physics and also interdisciplinary work in this area. The primary goal of this article is to bring this message to the general physics community.

(Some figures in this article are in colour only in the electronic version; see www.iop.org)

1. Introduction

Great progress has been made in the field of nanofabrication in the past twenty or so years. This fact is certainly well known to the readers of this journal. Most physicists are quite familiar with the impact of nanotechnology on many areas of condensed matter physics, including the physics of semiconductors, micro- (and nano-) electronics, and mesoscopic physics, not to mention the impact that this work has had on virtually all other areas of physics. While the vast majority of this work has been connected with electronic transport properties, nanotechnology is now being used to manipulate and elucidate other types of material properties. Indeed, most readers are probably at least somewhat familiar with the great progress which has been made in the area of microelectrical mechanical systems (MEMS). However, physicists are generally much less aware of the great impact which nanofabrication is now having in many areas of liquid-phase physics, chemistry, and biology. The extent of this work and its great promise for the future has not, in our opinion, gained the publicity it deserves in the physics community. The purpose of this review is to help generate some of this publicity.

For the purposes of this article we will organize this microfluidic work into five categories, which will be discussed in turn.

- (1) Early work on refrigeration and chemical analysis which led to some important applications, and anticipated many of the later developments.

-
- (2) Geohydrological work designed to provide insight into the flow of liquids in porous media, with a particular emphasis on percolation, viscous fingering, and related phenomena.
 - (3) Chemical applications in which very small volumes of reactants and products are manipulated, processed, and analysed.
 - (4) Biological experiments in which individual molecules, typically biopolymers such as DNA, are manipulated and probed.
 - (5) Studies of fluids in extremely small geometries, where the usual continuum and other ‘macroscopic’ approximations normally made in discussions of fluid behaviour would be expected to break down.

While the boundaries between these categories are not always clear-cut (especially with regard to the chemical and biological areas) this division is helpful in organizing this article.

We also will spend considerable time discussing the many ingenious fabrication methods which have been developed. While these methods build on what are now fairly routine nanofabrication techniques (and are thus likely to be familiar to many readers), we will see that some embellishments are needed in order to deal effectively with fluids. Unlike the solid layers used in nanoelectronics, fluids must be completely confined, so all three space dimensions of the structures must be considered with care. Moreover, it is generally much easier to move a measured number of electrons from one point to another than to do the same with a small volume of fluid.

A major goal of this review is to simply make physicists aware of the clever and important work being done in this field of microfluid mechanics. A second important goal is to point out areas where it seems likely that physicists could make significant contributions.

Before proceeding further, two disclaimers must be given. First, we will *not* spend any significant amount of time on the application of MEMS to fluid studies. There are already several very nice reviews of this area (reviews which emphasize fluids include references [1–4]). It will also turn out that such MEMS-oriented work is rather distinct in character from the microfluidic work upon which we wish to focus. Second, our review will be selective rather than exhaustive. Our goal is to convey the general flavour of what has been accomplished and where it might be heading, as opposed to assembling a voluminous catalogue. However, we have attempted to give an extensive set of references to aid the reader who wants to delve more deeply.

2. Fabrication overview

A microfluidic device must contain the fluid to be studied on all sides and provide for coupling the fluid into and out of this container. These basic functions have been accomplished in a variety of ways, using different types of materials and processing techniques. In this section we will give a rather general discussion of these methods and materials, as this will be helpful in appreciating the experiments described in the following sections. While additional details are also mentioned in connection with some experiments, a reader interested in the specifics is advised to consult the original papers.

A common approach is to build the microfluidic device ‘into’ a substrate, which is often either silicon or glass. The substrate is first coated with photoresist (or a functionally similar material), and the geometry of the flow structure is defined by suitable exposure of the photoresist layer to light. ‘Development’ of the photoresist (exposure to the appropriate solvent) then removes portions of the photoresist, thereby uncovering the substrate in selected regions (e.g., the regions where the photoresist was exposed to light). An etching process can then be used to attack the exposed regions of the substrate so that flow channels or similar

structures are produced in the body of the substrate. With silicon this can be done with a chemical etchant (e.g., anisotropic etching) or plasma etching may be employed. Both methods can produce extremely sharp and 'vertical' side-walls. With glass substrates the etchant is usually hydrofluoric acid. This tends to yield rather 'rounded' channel walls, which are nevertheless quite suitable for certain types of experiment. The microfluidic 'device' may consist of simple flow channels, but it is often the case that structures such as pillars or more complicated obstacles are arrayed within the flow channels, or that the channels are arranged in an intricate network. All of these possibilities and more can be accommodated with the patterning scheme described above.

The 'top' of such a microfluidic structure must be sealed, and this is often done with a glass cover-slip or microscope slide. With a silicon substrate, a bond between the glass and the silicon can be formed by gentle (~ 400 °C) heating while applying an electric field (of order 600 V) across the silicon/glass sandwich to ensure good contact via the associated electrostatic force; this method is known as field-assisted, or anodic, bonding. A glass substrate can also be bonded to a glass cover-plate by simply heating while applying a light pressure. With these bonding methods (and most of the other methods described in the next few paragraphs) the devices can usually withstand only modest pressures of a few atmospheres. In cases in which higher pressures must be tolerated, other bonding methods involving more conventional adhesives have been successful [5, 6].

A closely related approach is to begin with a substrate, typically glass, and again coat it with a layer of photoresist or some other light-sensitive material. This layer is then exposed to light and developed, as above, but now the remaining photoresist is left on the substrate and a cover-plate (again this is usually glass) is bonded onto the photoresist. This bonding can be accomplished by either gentle heating or by first applying a very thin additional photoresist layer to the cover-plate and then applying pressure [7]. This fabrication scheme is quite similar to the one described above in which the flow structure is etched into the substrate. The main advantage is that the flow structure is 'in' the photoresist layer, so no etching of the substrate is required. In addition, the side-walls of these photoresist channels are quite vertical.

A rather different approach, which has been recently developed by several groups, is to transfer the flow pattern into a thin flexible sheet, usually composed of a plastic-type material. The fabrication is straightforward (at least in principle), but requires several steps. In the implementation described by Lenormand [8] the flow pattern is first produced in a photoresist-like layer (essentially as described in the previous paragraph). This pattern is then transferred to a thin layer of polyester resin, and the top is ultimately sealed with a layer of wax [8]. The advantages of this approach are that highly vertical side-walls can be easily produced in a fully transparent structure (unlike silicon), and very large areas can be accommodated.

An approach which is similar in spirit but somewhat more 'flexible', has been described by Whitesides and co-workers [9, 10] (see also [11]). In their scheme, a raised pattern designed to serve essentially as a mould is first produced by either etching silicon or patterning a photoresist layer as outlined above. A thin layer of poly(dimethylsiloxane) (PDMS) is then cast onto the silicon surface where it assumes a shape which is the inverse of this mould. After curing, the PDMS layer can be removed from (peeled off) the silicon and then sealed to a smooth layer of glass, to a sheet of PDMS, or to any of several other materials [9, 10]. An advantage of this method is that the work of forming the pattern for the device need be done only once; a mould can be used and reused to produce many PDMS layers with precisely the same shape and dimensions. Such an approach is appealing when one wants to make many identical devices quickly and cheaply, and may well be the preferred method for mass production.

Regardless of which of these methods are used for forming the fluid container, one must allow for coupling the fluid in and out. This is typically done by building relatively large-area input and output regions into the microfluidic structure. These are usually regions of the device which are empty container regions, sometimes with pillars or posts to support the cover-plate. They are relatively large compared to the structure of the working parts of the device, so it is possible to contact them with macroscopic scale plumbing. This plumbing connection is usually made by drilling or etching a small hole through the substrate or cover-plate, and attaching a capillary with epoxy or simply an o-ring. It is not difficult to drill a 0.5 mm hole through a thin substrate, and typical inlet and outlet regions are several times larger than this.

The discussion in this section has been rather general, but will we hope illustrate the important common fabrication themes which have been developed by different groups.

3. Early work

Determining the beginning of a line or area of work is usually difficult and often subjective. It is also a good way to display one's ignorance and to become unpopular at the same time. Even so, we believe that two pieces of work which date from the 1970s are important ancestors to current microfluidic work. We will see that these ancestral experiments anticipated many of the important methods which are in common use today.

The first set of ancestral experiments was carried out by Little and co-workers [5, 6, 12, 13] in the development of refrigerators-on-a-chip. These papers are particularly nice as they begin with general questions on scaling of refrigerator size, and how this impacts the performance of basic components such as heat exchangers [6, 13]. This work led to a fully functioning and commercial refrigerator based on the Joule-Thompson cycle. These refrigerators use glass substrates and cover-plates. While silicon was investigated initially, it was not a suitable substrate choice, as its thermal conductivity is too high. As mentioned in the previous section, chemical etching of glass requires HF-based etchants which lead to rather rounded channels with poorly defined dimensions. To overcome this problem, Holman and Little used a 'sandblasting' method (literally) to etch the channels [5]. This etching method was not compatible with conventional photoresists, so an alternative gelatin-based photosensitive material was developed. While this etching method led to channels with fairly vertical side-walls, the channel bottoms were quite rough, and this prompted some interesting work on pressure-driven flow across rough surfaces [6]. The overall channel dimensions were typically 200 μm (wide) and 50 μm (deep). The roughness produced by the sandblasting was of order 20 μm , so this approach cannot be used to make significantly smaller channels (at least not without further refinements).

Bonding of the cover-plate also posed significant challenges. It is necessary for these refrigerators to withstand pressures of 200 atm, which is significantly higher than is common in most other microfluidic devices. This problem was overcome with a novel choice of adhesive [6], although this again limits the minimum channel depth.

The result of these efforts was a refrigerator-on-a-chip which can cool small samples to near 80 K in a few minutes, with the only external input being a source of high-pressure nitrogen gas. It is quite remarkable that the problems of etching glass with good side-wall definition, the development of an extremely durable alternative to conventional photoresist, and an approach to bonding which can withstand high pressures, were all solved so quickly and effectively. So far as we know, these devices were the first practical microfluidic devices.

Our second choice for ancestral work was carried out by Terry and co-workers [14, 15], who developed an essentially complete gas chromatography system on a chip, using a fabrication scheme quite similar to those currently in use. The flow channel geometry was defined by

chemical etching of a silicon substrate, with an anodically bonded glass cover-plate. A spiral flow channel was employed, with the inlet being an etched hole in the substrate at the centre of the spiral. The walls of this spiral channel were lined with a stationary phase. Perhaps most impressive was the implementation of a pneumatic valve to control the introduction of the gas mixture to be analysed, making this one of the earliest MEMS structures as well. In addition, a thin-film thermal conductivity sensor was used to measure the flux exiting the device. We should note that both the inlet valve and the thermal conductivity sensor were fabricated separately from the flow structure, and the three were then assembled. Hence, this was not a fully integrated device, as one might desire.

Not only did Terry and co-workers anticipate many important fabrication ingredients, they were able to assemble them into a device that actually worked, as they demonstrated successful separation of a mixture of hydrocarbon gases. It is a bit surprising that this work did not appear to lead to any direct successor activity, although it may have influenced Little. Perhaps it was just too different from what was then traditional, or more likely there was no recognized need at that time for such a device. Physicists built it, but no chemists came.

4. Geophysical devices

We now turn to what was perhaps the first major scientific application of microfluidic structures. This work continues at present, and involves the flow of one or more fluid phases through percolative microfluidic structures which are commonly referred to (in that subfield) as ‘micromodels’. Work in this area began nearly 20 years ago, with structures that were relatively large by today’s standards. Over time the percolative geometries have become more sophisticated, with smaller flow channels and obstacles, and the measurements themselves have become more quantitative.

A leader in this work has been Lenormand, but very substantial contributions have been made by a number of other groups. While this work involves problems near to the hearts of many physicists, including percolation, wetting, and fractal geometries, it has been targeted largely at (and published in the journals of) geoscientists, so it is not widely known or appreciated in the physics community. The volume of work is much too large for us to discuss all of it in detail here. Instead we will describe a few representative examples.

The microfluidic structures popular for geoscience studies have generally been made in two ways. One body of work [16–24] employs glass substrates into which the flow geometries are etched with HF acid. As noted in section 2, this tends to produce channels with rounded side-walls. One might view this as a major shortcoming, but some would argue that this is actually an advantage, since the flow geometries in real porous materials are likely to be rounded in similar ways. Another body of experiments [8, 25–27] have employed structures made using plastic/resin materials; as discussed in section 2, these flow channels have more precisely controlled dimensions and vertical side-walls. While this is certainly not typical of real porous materials, it is much easier to critically compare the behaviour of such idealized geometries with theoretical calculations.

Some of the earliest work in this area was by Lenormand and his collaborators, in which they explored percolation phenomena in flow systems like the one shown in figure 1. This figure shows a square-lattice network of channels which is suggestive of a bond percolation model (this particular sample was fabricated by the present authors). Lenormand and Zarcone [28] studied such structures in which the obstacles to flow were squares (as in figure 1) and were rather large, about 0.1 mm on a side. However, the overall device was also quite large, $30 \times 30 \text{ cm}^2$ (which must certainly be a record!), and their samples contained 250 000 such square posts arranged in a square array. The objective of this work was to investigate how

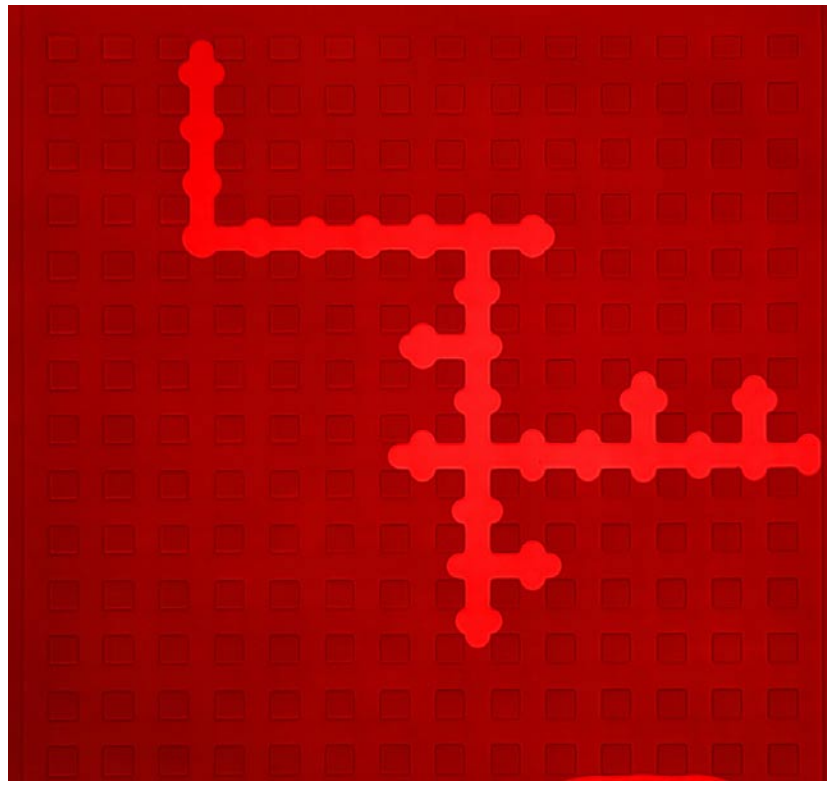


Figure 1. A flow network consisting of a regular array of obstacles. The obstacles are approximately square and $\sim 20 \mu\text{m}$ on a side; inlet and outlet regions are not shown. The lighter region is filled with air and is surrounded by silicone oil which is in the process of displacing the air that initially filled all of the open pore space. After [33].

a nonwetting fluid (in their case paraffin oil) displaces a wetting fluid (air), as the former is forced by pressure into the structure. This process was studied using photographs of the oil/air pattern as the air was slowly displaced. A second heroic aspect of this work was that the geometry of the invading oil network was measured by visual analysis of the photographs! The results showed that the invasion geometry was indeed fractal as expected on theoretical grounds, and the measured fractal geometry agreed well with the theory of invasion percolation with trapping effects included. Here ‘trapping’ refers to the fact that pockets of the wetting fluid can become surrounded as the nonwetting fluid invades. Once surrounded, the wetting phase is trapped forever.

Similar work by Lenormand and others has observed a variety of phenomena including percolation, viscous fingering, and diffusion-limited aggregation [8, 26, 27, 29, 30], and there is now a fairly good understanding of how the geometry of the flow structure leads to such different behavioural regimes. The precise geometrical control which is possible with lithographically defined flow structures has also been utilized in this work. For example, the effects of varying the amount of randomness in the percolative pattern has been studied using samples with log-normal channel size distributions [8].

All of the experiments mentioned so far in this section have been in good agreement with, and fully understandable in terms of, standard percolation theory and concepts. One might then ask whether this work has led to any new insights from a physicist’s perspective.

The answer to this is definitely in the affirmative, as illustrated by studies of the *dynamics* of how a nonwetting fluid displaces a wetting fluid in etched glass structures [18, 20, 31]. Of particular interest is the manner in which the wetting/nonwetting interface moves through a narrow channel. This is a dynamic process which can often be hysteretic, and often involves friction-like phenomena which are outside the scope of most percolation-based theories. An understanding of these processes is essential for understanding the geometrical arrangement assumed by the nonwetting phase during the invasion process. While the simplest percolation theory may be able to predict equilibrium behaviour (i.e., the idealized geometries assumed by the different phases), one must also understand the dynamics in order to know whether the system will actually reach equilibrium as opposed to becoming stuck in a nonequilibrium situation.

A valuable result of this line of work has been the opportunity to observe processes such as invasion *directly* and *visually*. To be able to see how the phases move, how interfaces become distorted, etc, can be extremely revealing. Recent work [22, 23] with etched glass structures has studied the motion of one or more invading fluids at the pore level using photomicroscopy. One interesting outcome of such work is an observation regarding the behaviour when the walls of the flow channels are somewhat rough [27]. It was found that a thin layer of the wetting phase can remain on the surface of a rough wall, even after the nonwetting phase has completely penetrated the central volume of the flow channel. That is, the nonwetting fluid can form a fully connected phase in the interior of the flow channels, while at the same time the wetting fluid forms a fully connected phase on the walls [20]. Hence, the two phases can flow simultaneously. This is, of course, an effect which cannot be described using the two-dimensional percolation models which have been used in the vast majority of theoretical analyses. Clearly, a treatment which has at least some three dimensionality will be required to describe such behaviour. It is doubtful that such behaviour would have been anticipated without the insight gained by direct visual experiments. Such visual studies have much untapped potential. For example, work on critical point wetting in random geometries [19] and related types of experiment on specially designed micromodels could yield interesting tests of our understanding of critical phenomena.

In more recent work with percolative flow structures, our group has studied flow rates through structures like the one shown in figure 2 [32]. The motivation for this work was the desire to provide a quantitative test of theoretical approaches for calculating the flow rates for fluids in porous materials. A completely first-principles calculation is not feasible, and various approximate numerical schemes have been developed. However, there is actually very little quantitative information available for carefully characterized microfluidic structures, so the accuracy of these theories is not really known. We [32, 33] have studied the pressure-driven flow of water through structures which were generated according to a particular fractal prescription [34] which is believed to be relevant to the geometry of the open pore spaces in fractured materials. Figure 2 shows an example of the flow geometry which was studied. The square obstacles are arranged as described by [34]; in this arrangement the coordinates of the squares are not quantized (i.e., discrete), and quite random patterns of overlapping squares are possible. The absolute flow rate was measured for a series of such structures, as the fraction of open-channel area was varied, and the results were compared with several computational approaches. As can be seen from figure 3, theory and experiment were found to agree at approximately the 10% level. The small differences between the two are believed to be due to uncertainties in the precise flow geometry. The fabricated flow pattern was not a perfect copy of the originally designed (intended) pattern; this can be appreciated from figures 1 and 2 where the ‘squares’ are seen to have slightly rounded corners, etc. When comparing with the theory, it was essential for the theoretical calculations to use the actual (measured) sample

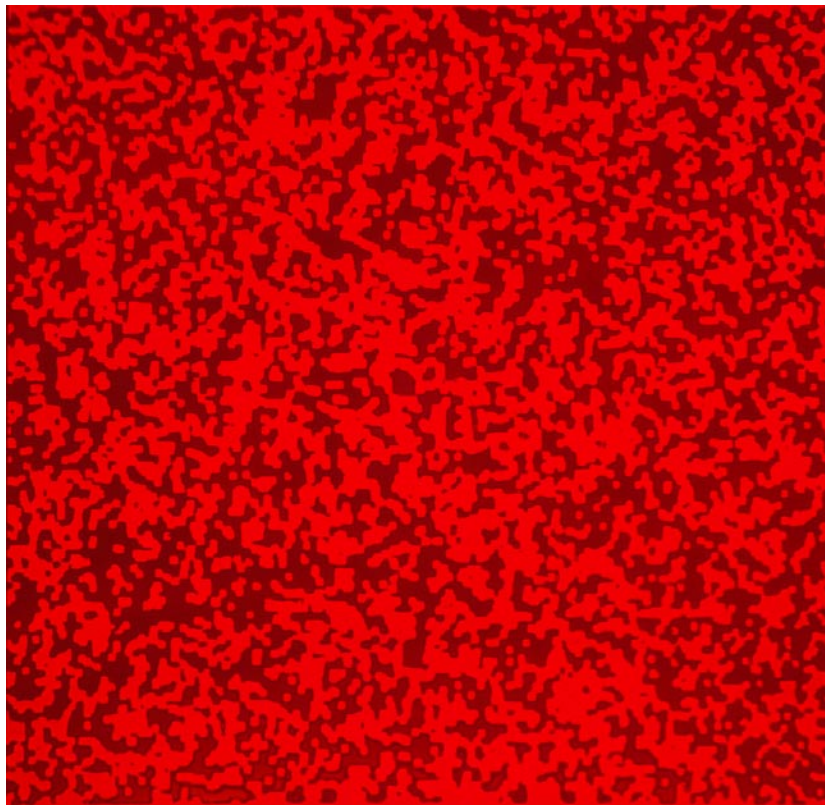


Figure 2. A flow network consisting of a random array of obstacles. The obstacles are approximately square (and $\sim 7 \mu\text{m}$ on a side) and are arranged according to the fractal scheme described by [34]. This scheme causes them to overlap significantly. From [33].

geometry, as determined via photomicroscopy after fabrication. The slight uncertainties in the measured geometry of open channels can account for the differences between theory and experiment in figure 3.

5. Chemical laboratories in small places

This section and the next are the areas in which microfluidic devices are now attracting the most attention, and both have enormous potential for new and interesting physics, as well as practical devices. The distinction between chemical analysis, which is the stated focus of this section, and more biologically oriented work involving individual molecules (usually biopolymers) which is the focus of the next section, is a bit blurry at times. Even so, this will provide a useful classification scheme for our discussion.

There are several reasons for wanting to make a small chemical laboratory on a microfluidic chip [35]. First, such a device would be able to work with extremely small volumes of reactants and products. This could be crucial when the available amounts are limited, or if one wants to be able to detect small numbers of molecules, as in a chemical sensor. Second, there is the possibility of processing a great many samples in parallel if one fabricates many reaction chambers and sensors on a single chip.

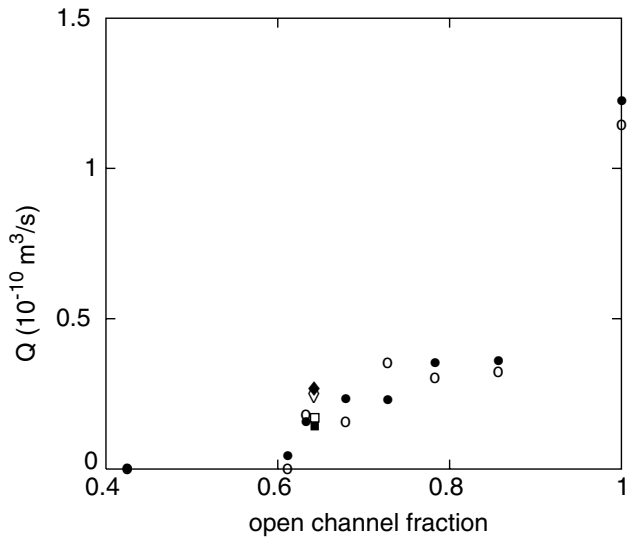


Figure 3. Measured (circles) and calculated (squares) results for the absolute rates of flow through random percolative flow structures like the one shown in figure 2. Open and closed symbols with a given shape at each value of the open-channel fraction give the theoretical and experimental values (respectively) for a particular sample. From [32].

We have already mentioned the early work of Terry and co-workers [14, 15] on a gas chromatograph on a chip. Their design essentially just scaled down a conventional macroscopic chromatograph. Indeed, a straightforward approach to chemical analysis with a microfluidic device might lead one to simply scale down the size of conventional devices, using the same working principles. While this approach may be appropriate in certain cases, it fails to account for a crucial way in which fluid dynamics differs in small geometries. Many key insights into these differences were discussed some years ago in an entertaining and insightful paper by Purcell [36], and the essential issues have recently been revisited in the specific context of microfluidics [37].

The crucial observation is that flow will almost always be laminar in the small channels found in microfluidic devices. Flow behaviour can generally be characterized by the Reynolds number, which (very roughly speaking) is the product of the channel size and the flow velocity divided by the kinematic viscosity. A Reynolds number somewhat greater than unity is necessary to produce turbulent flow. It turns out that viscous forces cause the Reynolds number in microfluidic structures to generally be much less than unity, making it essentially impossible to produce turbulent flow. One finds simple laminar flow instead. This observation is important for several reasons. For example, efficient mixing of two phases often relies on turbulent flow (e.g., stirring to mix the cream and sugar in your coffee), but this is not possible in microfluidic channels. In such small geometries the mixing will be diffusive, which may not always be desirable. On the other hand, it is possible to use the strong preference for laminar flow to one's advantage, as we will describe in our first example in this section.

Whitesides and co-workers have reported two experiments which illustrate the laminar nature of flow in microfluidic channels. In the first experiment two reactants were brought together in the simple flow geometry shown schematically in figure 4 [38] (for closely related work see reference [39]). Because of the laminar nature of the flow, the two fluids can flow side by side for quite long distances (many mm) with very little intermixing. This intermixing

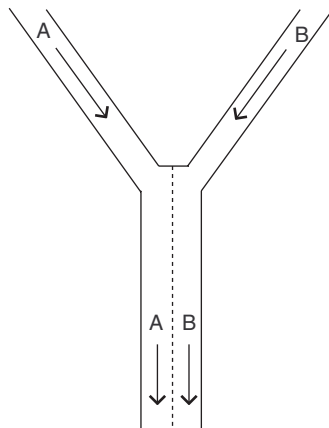


Figure 4. A schematic diagram of mixing/reaction geometry studied in reference [38] in which a fine metal line is laid down at an interface between two fluids flowing side by side in the same channel. Two fluids, A and B, enter through separate channels (top) and then leave through a single channel (bottom). The two intermix only over a narrow region, shown dashed, due to the slow nature of diffusive mixing.

will, as just noted, be diffusive so the thickness of the layer in which the two fluids are in fact mixed can be controlled to a large extent. In one example two fluids which reacted to form Ag were brought together [38]. This reaction only occurred in the mixing layer, and produced a Ag layer which coated the bottom of the flow channel. The width of the Ag layer thus gave a direct measure of the width of the mixing region. Interestingly, this procedure does not require a straight channel, and it is possible to deposit Ag lines around corners, etc. A number of other uses of this laminar flow mixing device have been demonstrated [38].

In subsequent work by the same group, the extent of the mixing region was studied in more detail using the structure shown schematically in figure 5 [40]. Here two inlet channels again merge into one outlet channel, with the inlets carrying two different fluids which reacted to form a fluorescent product. By monitoring the fluorescence, the spatial extent of the mixing region was obtained. Since the mixing is diffusive, the mixing layer would be expected to grow with time as $w \sim \sqrt{Dt} \sim \sqrt{z}$ where the connection to the downstream distance z follows from the assumption of a constant flow velocity. Such behaviour was indeed observed for fluid near the centre of the outlet channel. However, near the walls of the outlet channel (i.e., for x either large or small in figure 5) the mixing width was found to vary approximately as $t^{1/3}$. This result was shown to be understandable in terms of a scaling argument based on the Navier–Stokes equations; in words, the power law associated with this diffusive length scale is altered by the reduced fluid velocity near the channel walls [40].

This work carries an important message. In many microfluidic problems one is interested in reactions which take place on or near surfaces. One must think carefully about the nature of diffusive (and other types of flow) processes in regions where the flow velocity varies in space due to, e.g., the effect of a nearby boundary. As a ‘specific hypothetical’ example, the reaction rate for a chemical reaction which takes place on an interior surface of a microfluidic device may be strongly affected by diffusive transport. This point has also been emphasized from a theoretical point of view [41].

A potential advantage of microfluidic devices in the study of chemical reactions is associated with their very small reaction volume(s). If the dimensions of a reaction chamber are very small, it should be possible to start and stop reactions on very short timescales, and thereby

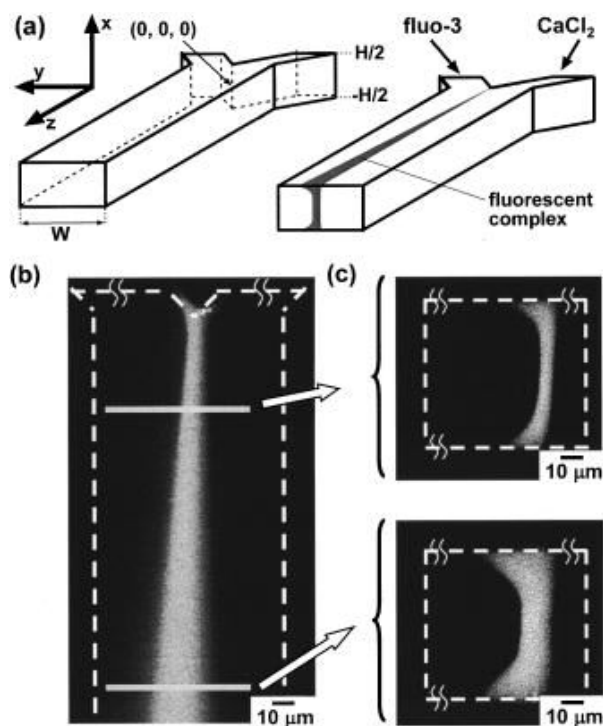


Figure 5. Top: microfluidic structure in which two fluids (labelled 'fluo-3' and 'CaCl₂') are brought together and leave through a common outlet channel. These two fluids react to form a fluorescent complex, and this fluorescence indicates the extent of the mixing region. Bottom left: a photomicrograph showing how the width of the mixing region grows as one moves downstream from the junction. Bottom right: photomicrographs showing that the mixing region is narrower in the centre of the channel than near the top and bottom walls. After [40].

perform time-resolved studies. However, we have just seen that mixing in these chambers is diffusive (i.e., slow), as compared to the ballistic process found in macroscopic cases. One way to overcome this problem is to make one of the dimensions of the reaction volume as small as possible. A clever way to accomplish this was described by Austin and co-workers, who devised the microfluidic geometry shown in figure 6 [42]. It is basically a focused nozzle, in which the focusing is controlled by two transverse fluid beams. The inlet channel on the left is shaped as a nozzle and emits a beam of one fluid which appears as lightly shaded in the figure. Two transverse channels of uniform cross-section enter the nozzle region from above and below in figure 6, and the channel to the right carries the output.

Figure 7 shows how this device focuses the central fluid jet. These are actual results (not a simulation); the optical contrast is obtained by using the fluorescence of the fluid in the central beam. The extent of the focusing, i.e., the width of this central jet of fluid, is adjusted by varying the pressures of the top and bottom focusing beams in figure 6 relative to the inlet stream. In this way the thickness of the outlet beam could be made as small as 50 nm [42]. In a mixing application the inlet beam would contain one of the reactants while the other reactant might be in one (or both) of the focusing fluid streams. The thickness of the effective reaction region would then be that of the focused beam, so a narrow output stream will speed up mixing. In the devices studied in reference [42] the mixing times were less than 10 μs. This approach to mixing should have applications in time-resolved studies of chemical reactions.

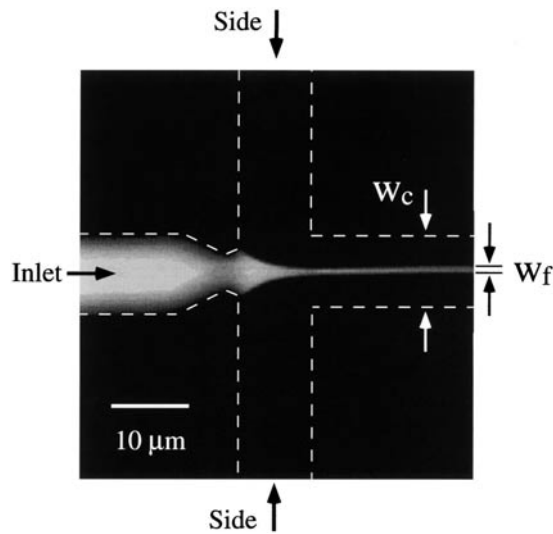


Figure 6. Microfluidic geometry used to enhance mixing. This is a photomicrograph of a fluorescent liquid as it moves from the left (from the region labelled ‘Inlet’) to the right. The dashed lines show the boundaries of the flow channels (which are not evident in the micrograph). Nonfluorescent liquid flows into the central region from the top and bottom (from the regions labelled ‘Side’) and causes the inlet beam to be focused, so the output beam is extremely narrow (W_f) compared to the width of the outlet channel (W_c). After [42].

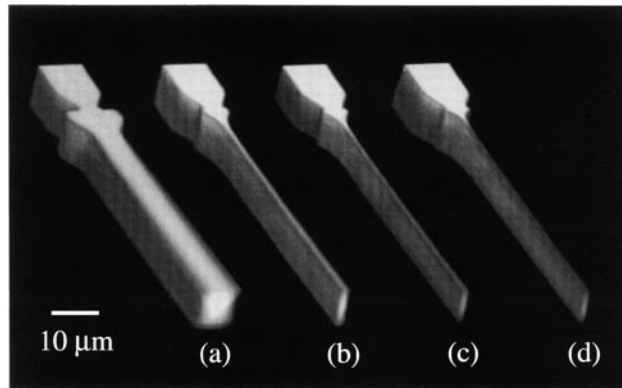


Figure 7. Photomicrographs of focused beams produced from the microfluidic device in figure 6. The beam of focused liquid is made visible by its fluorescence. The photomicrographs labelled (a)–(d) show results with different ratios of the side to inlet pressure. After [42].

A more ‘brute-force’ type of solution to the problem of mixing has been described in references [2, 43]. They produced a device in which one of the reactants is injected into the reaction chamber through an array of small nozzles. While each of these nozzles was relatively large (15 μm in diameter), there were a lot of them (several hundred), so the mixing time was reduced accordingly.

Let us now consider a process which is the inverse of mixing, namely separation. Chromatography is a key component in analytical chemistry; it is often implemented with macroscopic capillaries packed with a powder which makes the surface area within the capillary

very large, and this surface area is then coated with a stationary phase. It is difficult to use a ‘mechanical’ method to efficiently pack a powder into the flow channel of a microfluidic device. Many workers (e.g., [14, 15]) have simply used a narrow channel and omitted the powder; the stationary phase can be synthesized *in situ*, by injecting two fluids which react to form the desired material (for a different approach involving microfluidic structures see reference [44, 45]). However, Regnier and co-workers have shown that much improved performance could be attained if these channels could be filled with something like a powder. They developed an approach to this problem which is illustrated in figure 8 [46, 47]. The basic idea is to fill a flow channel with an array of pillars, which here are rectangular. In this device the substrate was quartz and reactive-ion etching was used to obtain very sharp and vertical side-walls, as can be seen from figure 9. In a sense, this is the ideal powder; it is quite small but also very uniform in its dimensions. Moreover, the pillar shape, size, and spacing can all be controlled with great precision, and can be tailored for optimal performance. In the work of He *et al* [46] these chromatography ‘columns’ were coated with a stationary phase *in situ* (by pumping suitable reactants into the flow chamber), and their performance has been studied in detail [46].

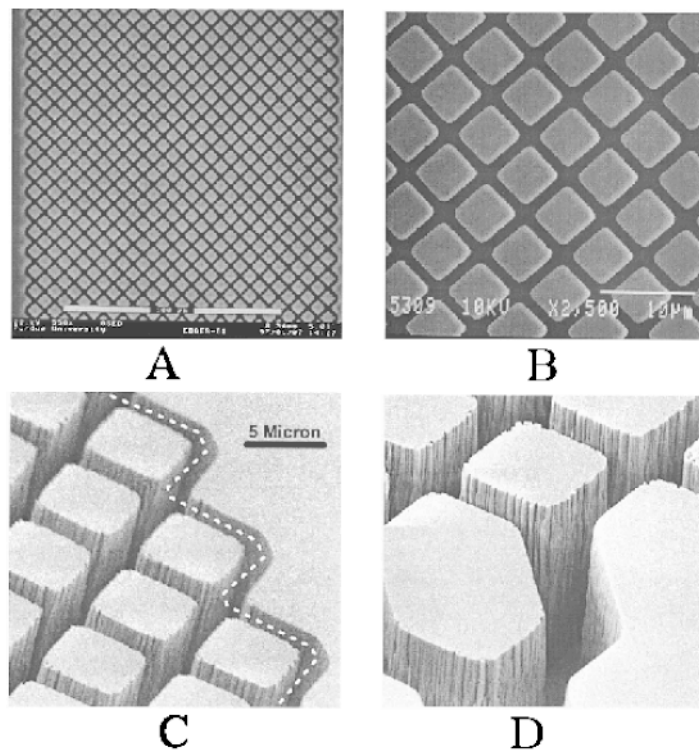


Figure 8. Scanning electron micrographs of an array of posts designed for use in chromatography. After [46].

The micrographs in figure 8 remind one of a filter. Indeed, filters are essential for many microfluidic applications. A straightforward and obvious way to make a filter is to simply put obstacles like the pillars in figure 8 into a flow channel, with the spacing between pillars chosen according to the desired filter properties. However, while it is certainly functional, this approach is perhaps a bit too simple, since such two-dimensional structures are much more

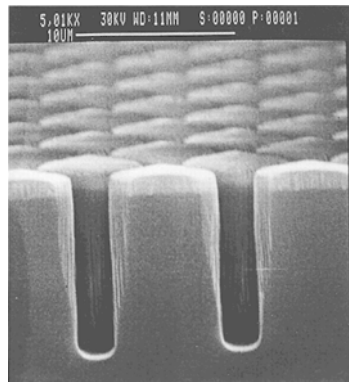


Figure 9. A scanning electron micrograph showing a side view of the channels from figure 8. The channel walls are seen to be quite 'vertical'. The substrate is quartz, and the channels were produced with reactive-ion etching. After [46].

prone to blockage than three-dimensional geometries. Structures in which the flow is three dimensional make much better filters. Regnier and co-workers [48] have shown how to obtain such a flow geometry as part of a microfluidic device. The key is to make the filter as part of the inlet to the device. We have not spent much time discussing how one couples fluid into or out of microfluidic structures. Typically one simply drills or etches holes into either the substrate or the cover-plate, and attaches quasi-macroscopic capillaries. The flow field must therefore change from three to two dimensional where the capillaries attach; it is in this region that the filter structure shown schematically in figure 10 is located. Here a fluid containing the particles to be filtered enters from above through an inlet capillary which is not shown, and exits laterally. Particulates are trapped on the tops on the pillars, while the fluid is able to flow around and below the trapped particles. This separation of the trapped particles from the flow region, through the use of effectively two separate flow layers, gives significantly better performance than a purely two-dimensional design (such as a simple array of pillars). This

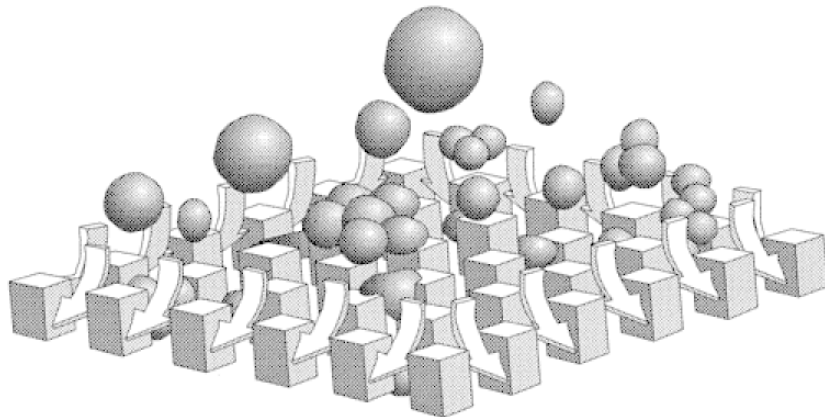


Figure 10. A schematic diagram of quasi-three-dimensional filter action at the inlet to a microfluidic device. The spheres depict particulates which are to be caught in the filter. These particulates enter (with fluid) from above, and the fluid flows out laterally as indicated by the arrows. After [48].

approach is at least a partial solution to the problem of filtering in microfluidic devices. We use the term ‘partial’ since such filters can only be used at the inlet to the device; they cannot be inserted at arbitrary locations. On the other hand, if the fluid is well filtered on entering the device, subsequent filtering may not be necessary.

So far we have generally assumed (at least implicitly) that the fluid is driven through the microfluidic device by an applied pressure. It is also possible to use an electric field to drive or control flow through a device, using the electro-osmotic effect (EOF). This is nicely demonstrated by the structure shown in figure 11 [49]. Here there is a single inlet channel which enters from the left, and two outlet channels through which fluid or molecules can exit to the right. In addition there are two more channels which enter transversely, here from the top and bottom. These top and bottom channels are not used to transport fluid directly, but rather to impose a transverse force on the fluid entering from the left. Hence, this device acts as a switch which can control the path taken by a neutral fluid, or perhaps ions or molecules, which enter from the left.

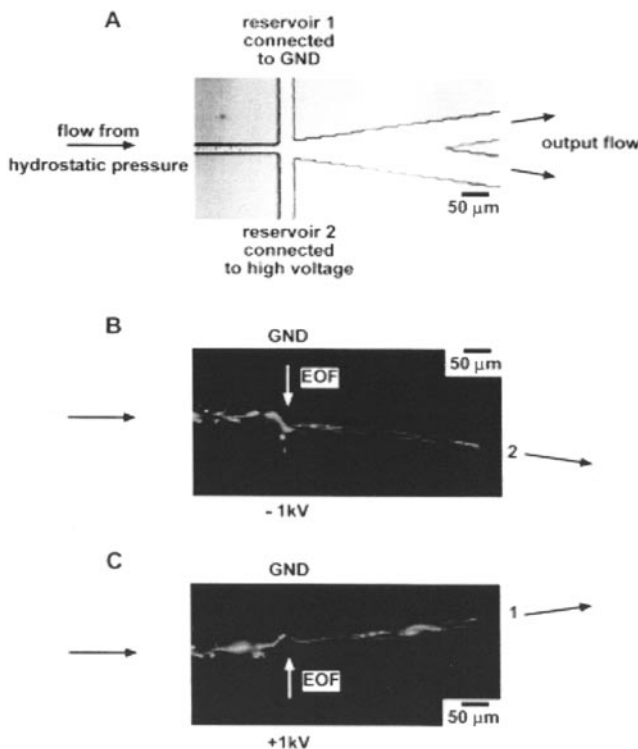


Figure 11. Top: flow geometry which can be used as a deflection switch. Fluid entering from the left reaches the junction region at which channels from the top (reservoir 1) and bottom (reservoir 2) join. By applying a pressure difference or an electric field between the two reservoirs, the inlet stream can be deflected into either the upper or lower output channel as indicated on the right. This device was fabricated from the plastic PDMS. Bottom: micrographs showing a fluid stream deflected either down (in part B) or up (part C) using an electric field. The fluid was made visible through its fluorescence. After [10, 49].

In the experiments [49] the inlet fluid contained small ($1 \mu\text{m}$) plastic beads containing a fluorescent dye, which allowed their motion to be tracked. In some experiments the transverse force used to steer (i.e., switch) the beam into one of the two outlet channels was provided

by applying a pressure between the two reservoirs (labelled 1 and 2 in figure 11). However, a more convenient way to apply this switching force is to use an electric field and take advantage of the EOF [50]. The EOF arises from the fact that the surfaces of a flow channel are generally charged, or can be made so with a suitable coating. In the device in figure 11 they were negatively charged, which produced a layer of positively charged ions next to the surfaces. This charged layer can be made to move by the application of an electric field, dragging neutral fluid along with it; this is the EOF [50].

Returning to figure 11, some results are shown in which the EOF was used to produce the switching force. While successful operation was thus demonstrated, it does not appear that this device is ready for routine operation. The electric potentials required were relatively large, with 1 kV applied across the control reservoirs. In addition, there was also some probability that the incoming beam of plastic beads would be deflected into one of the control channels. It seems likely that these problems can be overcome, perhaps by suitable reduction of the device dimensions, and the use of metallic leads on the channel walls to apply the necessary electric field.

In this section we have focused on the design and operation of a few of the basic components necessary for the implementation of a chemical laboratory on a chip. Several groups have shown how to assemble these components to produce complete on-chip laboratories. Some workers have pursued liquid chromatography with an open-tube column (i.e., a column without any powder) [15, 51]. A number of groups have produced chips for capillary electrophoresis, perhaps because this approach uses an electric field to drive the sample through the device so no high pressure need be applied [44, 45, 52–56]. These devices have been used in a variety of separation experiments, including many involving biopolymers. In addition, several other interesting devices designed to separate and analyse small volumes of biopolymers have been demonstrated [57, 58].

6. Biophysics and the manipulation of single molecules

The chromatography columns discussed in the previous section operate in a manner which is similar, at least in spirit, to that of conventional columns. A ‘pulse’ of fluid is injected into the column and the flux of molecules out of the column is measured as a function of time. Separation then occurs because different molecules have different mobilities and thus exit at different times. However, it has been shown [11, 59–61] that microfluidic devices can separate molecules according to their mobility in a rather different manner, which has been given the provocative name ‘rectification of Brownian motion’. (See also the very interesting and related work on the motion of polymer chains through an array of obstacles in references [62–64].) Consider again a flow channel filled with an array of obstacles, but imagine that the obstacles are ‘left-right’ asymmetric with respect to the driving force as shown in figure 12. Here an electric field directed downwards in the figure is used to drive DNA fragments through the obstacle course [11]. While the electric force will give rise to an (approximately) constant velocity along the field direction [36], there will also be diffusive transverse motion of the DNA. There will thus be some probability for a molecule to move to the right or left in the open regions between obstacles. The asymmetries in the obstacle course, i.e., the shapes and geometric arrangement of the obstacles, will make the right- and left-going probabilities different; in this particular device, there will clearly be a greater probability to move to the right. Let P_R and P_L be the probabilities that a molecule will diffuse one ‘lattice spacing’ to the right or left as it travels between consecutive rows of obstacles. If for all molecules P_L is much less than unity (due to the asymmetry in the obstacle course), then molecules will not move in significant numbers to the left. The right-going probability P_R will depend on the

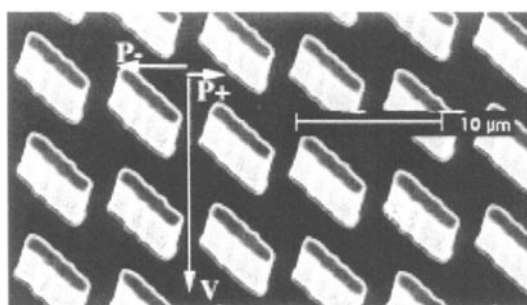


Figure 12. A scanning electron micrograph of a flow region which contains an array of obstacles. Molecules (actually ions) are driven through the device by an electric field directed from top to bottom. The key point is that the obstacles exhibit left-right asymmetry with respect to the direction of the electric field. After [11].

diffusion constant of a molecule, and we would generally expect it to be larger for smaller molecules and vice versa. If a molecule is small and P_R is thus large, the molecule will tend to diffuse a large distance to the right as it travels through the device; a large molecule with a small P_R will diffuse a much shorter distance to the right. Hence, the rightward displacement will depend on molecular mobility, with different molecules emerging at different locations from the device.

Figure 13 shows the paths taken through such an obstacle course by DNA fragments of differing length. As expected, the larger fragment moves relatively little to the right, while the short fragment is deflected more. In a conventional chromatography column the separation is in the time domain, but in such an asymmetric obstacle course there is a spatial separation. This ‘Brownian’ sorting device can thus operate continuously in time, which may be advantageous [11].

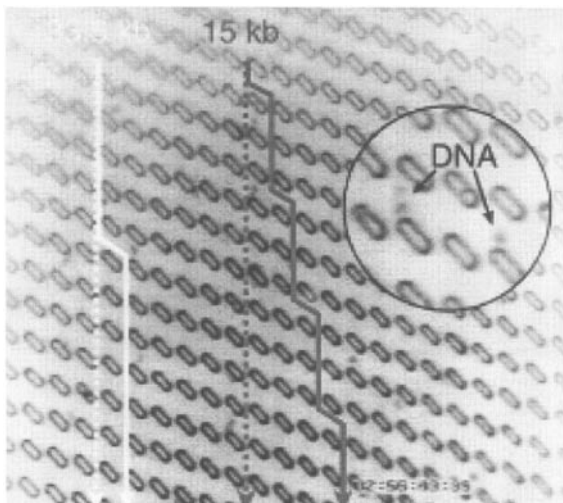


Figure 13. Motion of DNA fragments driven through an obstacle course like that shown in figure 12. After [11].

Most of the chemical and biological microfluidic devices discussed so far are, roughly speaking, designed to move fluids or molecules from place to place. However, there is also the possibility of probing the structure of a molecule as it moves through a device. One way in which this can be accomplished has been demonstrated by Austin and co-workers [11, 64]

who have tailored a flow geometry in which molecules are driven by an electric field through a long narrow flow channel, as shown in figure 14. The flow channel itself is completely open; it contains no obstacles, but the bottom of the channel is an opaque metal layer which contains several very narrow slits (here of order $1 \mu\text{m}$ or less in width) which run perpendicular to the channel. When a laser beam illuminates the opposite side of the metal layer, an optical field is established within the flow channel in the region immediately adjacent to each slit. In these demonstration experiments, either DNA molecules labelled with a fluorescent complex or small plastic spheres labelled in a similar manner were driven through the channel using an electric field [11]. When such a labelled marker passes over a slit it will fluoresce and can thereby be detected. The time dependence of the fluorescence signal then contains information about the location of particular portions of the molecule as a function of time. In some respects, this very clever design was anticipated by DeBlois and Bean [65], who also studied the flow of small ‘things’, such as viruses, as they moved through narrow channels. DeBlois and Bean monitored the motion of individual virus particles by measuring their effect on the conductivity of the channel (which contained an electrolyte); they thus had no way to get spatial information.

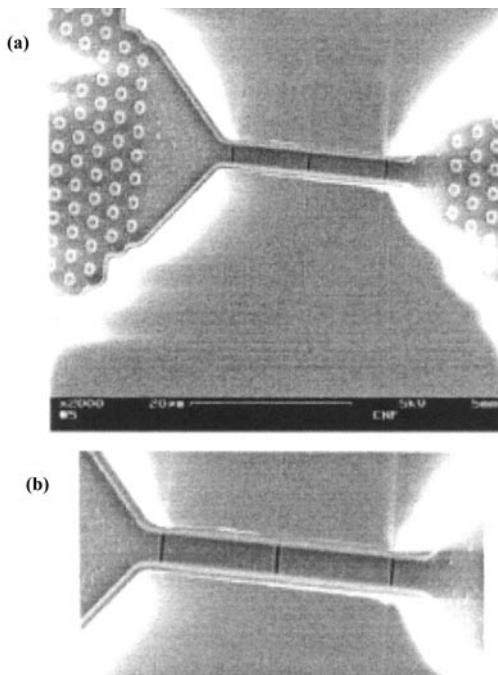


Figure 14. Top: a narrow ($\approx 3 \mu\text{m}$) flow channel connecting two wider regions containing pillars (the circles at the far left and far right). The central narrow channel passes over three narrower ($0.1 \mu\text{m}$) transverse openings (slits) in an opaque underlayer of aluminium. A laser is used to provide illumination through the transverse slits; the portion of a molecule which is located over a slit is thus probed by the laser. Bottom: an expanded view of the central portion of the device. After [11].

In the microfluidic device shown in figure 14 the molecules passed through an inlet region containing a symmetric array of posts, prior to entering the channel [11]. This caused some of the molecules to be elongated somewhat (at least compared to a completely coiled conformation) as they moved along the channel. Ideally, one would like a polymer chain to completely uncoil and move through the channel as a long straight chain. If this can be made to occur, then

the device in figure 14 could conceivably be used to make spatially resolved measurements on specific portions of the polymer chain, and perhaps even perform direct sequencing. Such measurements will likely require significant reductions in the size of the microfluidic device. Narrower channels will be needed so that the molecules will assume an uncoiled state, and sequence-level spatial resolution will probably demand much narrower slits. However, such reductions in size seem feasible. This sort of microfluidic device is just one example of the way that molecules can be probed when the device dimensions approach the molecular regime.

7. Just plain physics

In this section we will discuss a few examples which do not fit neatly into any of the categories considered above, but which we feel illustrate some other important kinds of issue which can be addressed with microfluidic devices.

Essentially all of the flow structures discussed so far are two dimensional. It would clearly be of interest to assemble structures which are three dimensional or, failing that, structures containing multiple flow layers. Some progress in this direction has been made [66], but the designs which have been implemented to date involve only two layers and require a critical alignment step which may make scaling to smaller scales problematic (roughly speaking, in the work carried out so far, two separate substrates, each containing flow channels, are bonded together). The fabrication of truly three-dimensional flow structures is clearly not a simple task, and we see it as one of the major challenges facing the field of microfluidics.

Another way to access the third dimension in microfluidic devices was pointed out in reference [67]. Their approach makes clever use of electro-osmotic effects (EOF). We have already mentioned that a very convenient way to drive molecules and also neutral fluid through a microfluidic device is with the EOF. This effect exploits the fact that the walls of a microfluidic device are generally charged; one could certainly imagine controlling the surface charge by coating the walls with a conducting layer, or one can coat insulating walls with particular chemical species. Stroock *et al* have taken this a step further by depositing a *patterned* charge density on the inner walls of a flow channel, as illustrated in figure 15. They have considered two cases, one in which the charge density on the walls varies transversely to the applied electric field, and another in which it varies along the field direction. To appreciate the manner in which this will affect the flow, consider first the transverse case as shown at the top of figure 15. Here there is a positive charge density on the bottom surface of the flow channel and a negative charge density on the top. We will not go into the methods used to apply these charge densities here, but only note that they involve the selective deposition of organic polymers onto the walls of the flow channel [68–71]. Without any applied electric field the surface charges in figure 15(a) will attract a layer of positive ions to the top of the channel and a layer of negative ions to the bottom. An electric field applied along the $+z$ -direction will cause these ions to move, and since they are oppositely charged they will move in opposite directions. As they move they will drag with them the uncharged fluid, and thereby set up a counterflow pattern, with fluid at the top and bottom of the channel moving in opposite directions and the middle region undergoing shear flow.

An even more interesting flow pattern is created when the charge density is modulated along the direction of the applied electric field, i.e., along z in figure 15(b). This electric field will now cause the fluid to move in circulating rolls which alternate in polarity along the z -direction. Figure 16 shows experimental results obtained for this case. The flow velocity was measured by seeding the fluid with fluorescent plastic spheres. Microfluidic structures of this type may prove very useful in devising new approaches to the mixing of fluids and to manipulating the motion of molecules.

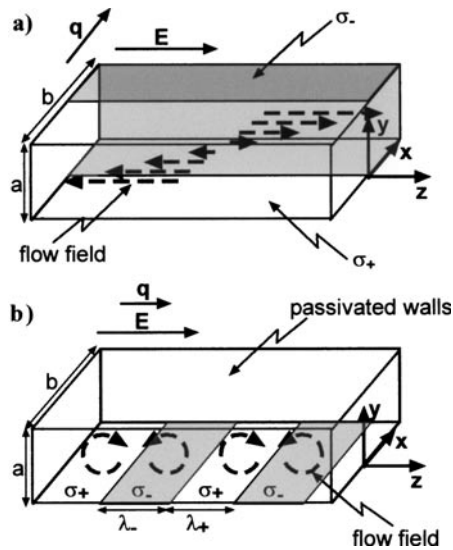


Figure 15. A schematic diagram of the charge patterns deposited onto the interior walls of a flow channel. In (a) a positive charge is applied to the bottom wall and a negative charge to the top. An electric field directed to the right then drives the fluid as shown through the electro-osmotic effect. In (b) the charge density on the bottom wall varies in sign along the flow direction, and which leads to a more complex velocity field. After [67].

The microfluidic devices which we have described so far are not particularly small by the standards of what can be achieved today with ultrahigh-resolution lithography and thin-film techniques. Current state-of-the-art lithography can achieve feature sizes as small as $\sim 10\text{--}20$ nm, and very uniform (solid) films can be made much thinner than this. Such small dimensions are not required or necessarily desirable for many microfluidic applications. However, they are of interest with regard to several basic questions concerning the physics of simple liquids. For example, the usual treatment of fluid flow near a solid surface assumes that the tangential velocity vanishes at the surface. This assumption may be adequate at macroscopic scales, but we certainly do not expect it to give an accurate quantitative description of flow very near a surface. This picture can be made somewhat more realistic by allowing for a slip length, but one would still like to understand how to calculate the magnitude of this length from fundamental theoretical principles. Moreover, adding a nonzero slip length to the description is probably not enough; one would expect to also find spatial variations in the fluid density near a wall, etc. Such effects should have profound consequences for fluid flow near a wall. This is a problem which is difficult to tackle theoretically, but some progress is being made, especially with molecular dynamics simulations [72–74]. On the experimental side there has been work on how confinement in a small container can greatly alter many of the static (i.e., structural) and dynamic properties of a fluid [75]. Many of these experiments have employed open geometries in which two extremely flat surfaces which are immersed in a ‘bath’ of the fluid are made to come nearly into contact [76–79]. Other experiments have used optical methods to probe the flow velocity near a surface in a macroscopic container [80, 81].

A much simpler experimental approach to this problem, at least in principle, is to study the behaviour of a fluid in a very small container, i.e., in an ultrasmall microfluidic channel. Such a device must be very small since the slip lengths for most fluids are expected to be of order a few molecular diameters. Several groups have conducted such experiments, with mass flow

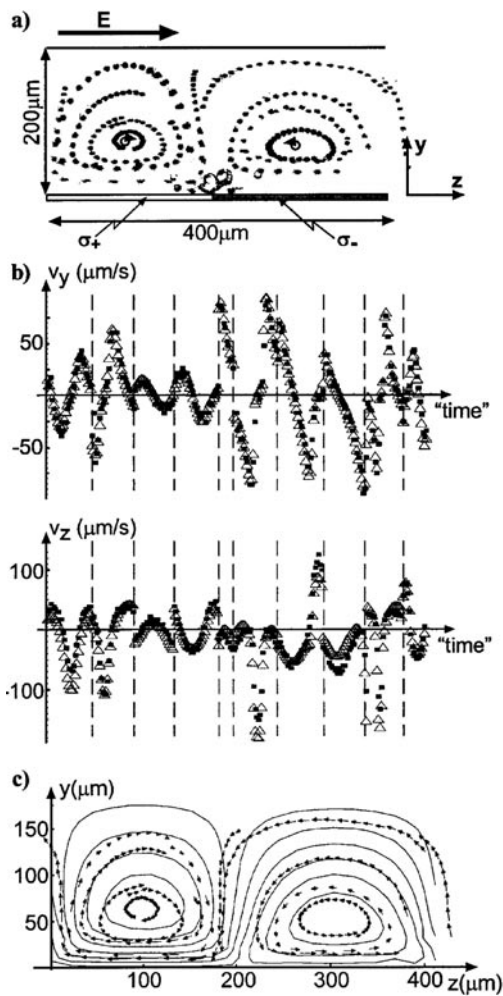


Figure 16. Measured velocity fields in the flow channel shown in part (b) of figure 15. The velocity field exhibits ‘rolls’ whose axes are perpendicular to the electric field (along x in the figure). The polarity of the rolls alternates as one moves along z . The solid lines in (c) show calculated velocity fields, while the arrows here, and the data in (a) and (b) are all experimental results. The flow velocity was measured by seeding the fluid with fluorescent plastic spheres. After [67].

measurements of both liquids (see the references below) and gases [82–84], and also studies of heat conduction. Here we will focus on studies of the pressure-driven flow of simple liquids.

While many workers have studied the absolute flow rates in pressure-driven (Poiseuille) flow (for example [6]), the first microfluidic search for deviations from the ‘simple’ theory, i.e., the theory assuming no-slip behaviour at the boundaries of a microfluidic flow channel, was reported by Bau, Zemel, and co-workers [85–88]. In a series of experiments they studied the flow of various fluids including several alcohols, water, and silicone oil. In our view, the results were inconclusive; in some cases the measured flow rates were larger than predicted by the theory, while in other cases the flow rates were lower. There was no discernible pattern, and in some instances nominally similar flow channels gave different results. The reasons for these variations are still not clear, despite much effort in characterizing the flow channels, especially

their roughness. These experiments are not easy; the Poiseuille flow rate varies (theoretically) as h^3 , where h is the height of the flow channel (we assume here that the channel is much wider than h , as was the case in these experiments). Hence, a rather small uncertainty in h leads to quite significant uncertainties in the theoretically expected flow rate. We should also note that the channels studied by Bau, Zemel, and co-workers had $h \sim 0.5 \mu\text{m}$ or larger. According to the theory, no measurable deviations from the theory would be expected in such thick channels.

In very recent work, we have studied Poiseuille flow in substantially thinner channels, with h as small as 30 nm [7, 33]. In order to get an independent check on the value of h , we have filled the channels with an electrolyte (usually a weak acid) and measured the conductance using metal film electrodes deposited in the inlet and outlet regions adjacent to the channel. Our best estimate is that our uncertainties in h are of order 5%, so comparisons with the theory can be made at approximately the 15% level. Another important experimental consideration concerns the measurement of the flow rate, Q . Since as noted above $Q \sim h^3$, our extremely thin channels exhibit very small values of Q . In the thicker channels studied previously [85–88] it was feasible to measure Q by observing the flow through a macroscopic capillary which was connected in series with the flow channel. This is not practical when h is below a few hundred nanometres. In our work we have measured Q *in situ* on the microfluidic chip in one of two ways. First, we observed the fluid as it entered and moved through the channel, using straightforward microscopy. Second, in some experiments we fabricated a second larger (wider and deeper) flow channel in series with the narrow channel of interest, and measured the flow (again using microscopy) through this larger channel.

Some results for several fluids are shown in figure 17. For water there may perhaps be a slight increase in $Q(\text{exp})/Q(\text{theory})$ at the smallest values of h , but to within the approximately 15% uncertainty there is no firm evidence for any deviation from the flow rate calculated assuming no-slip boundary conditions, even for our smallest channels. However, for hexadecane we find greatly enhanced flow (as compared to the no-slip calculation) for h

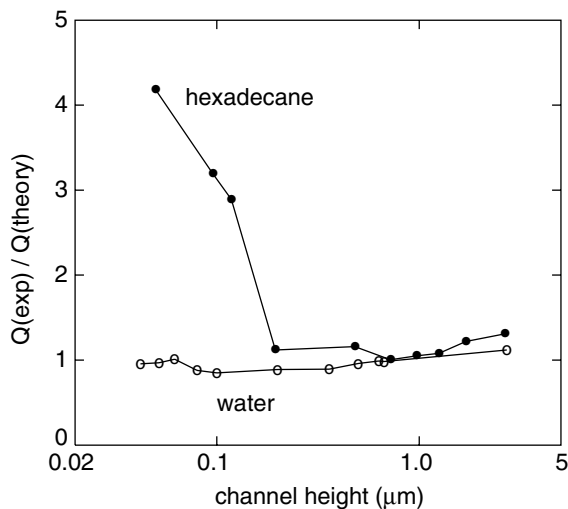


Figure 17. $Q(\text{exp})/Q(\text{theory})$ as a function of channel height h for pressure-driven flow through channels with rectangular cross-sections. Here $Q(\text{exp})$ is the experimentally measured volume flow velocity per unit pressure, while $Q(\text{theory})$ is the corresponding theoretical value calculated from Poiseuille's law assuming no-slip boundary conditions. The channel width was much greater than h . After [7].

below about 100 nm. This is in agreement with other work on hexadecane in which optical measurements were used to study the fluid velocity near a wall [80, 81]. Our method has the possibility of much greater spatial resolution, and it may also be feasible to observe the predicted non-Newtonian effects [73] in this regime of very small h . Such experiments are now in progress.

8. Summary and outlook: what does the field need and where is it heading?

This article has contained a very rapid tour of the field of microfluidics. Space has not allowed us to go deeply into the experimental details, but we have tried to give a representative glimpse of the novel and creative types of structure which have been constructed. In closing we would like to mention what we see as particular challenges and opportunities for significant further advances.

First, it would be extremely interesting to devise a way to fabricate three-dimensional, or at least multi-layer microfluidic devices. So far as we are aware, no one has demonstrated an integrated structure in which two (or more) flow channels are able to cross each other. Here we do not count structures in which flow channels are in two separate substrates which are then bonded together [66] (even though this is very nice work!); we exclude these approaches, because we do not see how such double-layer structures can be scaled down to much smaller dimensions.

Second, there is a pressing need for new types of sensor and on-chip measuring device. In many of the demonstration experiments described in this article, fluorescence was used to follow the motion of molecules or small plastic seed particles which were suitably tagged with a fluorescent complex. While this is certainly a powerful technique, there is a need for probes which do not require specially prepared or tagged targets, and which do not rely on microscopy to obtain spatial resolution, and for new types of sensor in general. This is an area where we believe that physicists can make major contributions. For example, one could imagine small optical sensors integrated into a microfluidic device so as to permit spatially resolved measurements at many locations simultaneously. Or, one could use inelastic (electron) tunnelling spectroscopy to discriminate between different molecular species as they pass through a tunnelling volume. Such sensors could be very small, and many could be distributed throughout a microfluidic device.

We hope that the physics community will take up these challenges. We are convinced that microfluid mechanics provides many interesting directions for future research.

Acknowledgments

We thank D D Nolte, L J Pyrak-Nolte, and P F Muzikar for many helpful discussions, and G A Fiete and M R Dorbin for their valuable participation in our initial experiments in this field. We also thank R H Austin, F Regnier, A D Stroock, and G M Whitesides for permission to show their results, and for kindly providing them in a convenient form for reproduction. Our work in this field was supported by NSF grant DMR-9970708 and DOE contract DE-AC26-99BC15207.

The following list of references is intended to be representative, and we believe that it is reasonably complete. However, this field is so large that we cannot guarantee that this list is exhaustive, and we apologize to anyone whose work we have omitted. We hope that this list will give the interested reader a good start in tracking down the work that has been done in any particular area of interest.

References

- [1] Gravesen P, Branebjerg J and Jensen O S 1993 *J. Micromech. Microeng.* **3** 168
- [2] Elwenspoek M, Lammerink T S J, Miyake R and Fluitman J H J 1994 *J. Micromech. Microeng.* **4** 227
- [3] Gad-el-Hak M 1999 *J. Fluids Eng.* **121** 5
- [4] Löfdahl L and Gad-el-Hak M 1999 *Prog. Aerospace Sci.* **35** 102
- [5] Holman R and Little W A 1981 *Refrigeration for Cryogenic Sensors and Electronic Systems* NBS Special Publication 607, ed J E Zimmerman, D B Sullivan and S E McCarthy (Washington, DC: US Government Printing Office) p 160
- [6] Little W A 1982 *Physica B* **109+110** 2001
- [7] Cheng J-T and Giordano N 2001 to be published
- [8] Lenormand R 1989 *Physica D* **38** 230
- [9] Duffy D C, McDonald J C, Schueller O J A and Whitesides G M 1998 *Anal. Chem.* **70** 4974
- [10] McDonald J C, Duffy D C, Anderson J R, Chiu D T, Wu H, Schueller O J A and Whitesides G M 2000 *Electrophoresis* **21** 27
- [11] Chou C-F, Austin R H, Bakajin O, Tegenfeldt J O, Castelino J A, Chan S S, Cox E C, Craighead H, Darnton N, Duke T, Han J and Turner S 2000 *Electrophoresis* **21** 81
- [12] Little W A 1978 *AIP Conf. Proc.* **44** 421
- [13] Little W A 1981 *Refrigeration for Cryogenic Sensors and Electronic Systems* NBS Special Publication 607, ed J E Zimmerman, D B Sullivan and S E McCarthy (Washington, DC: US Government Printing Office) p 154
- [14] Terry S C 1975 *PhD Thesis* Stanford University, CA
- [15] Terry S C, Jerman J H and Angell J B 1979 *IEEE Trans. Electron Devices* **26** 1880
- [16] Wardlaw N C 1982 *J. Can. Petrol. Technol.* **21** 21
- [17] McKellar M and Wardlaw N C 1982 *J. Can. Petrol. Technol.* **21** 39
- [18] Li Y and Wardlaw N C 1986 *J. Colloid Interface Sci.* **109** 473
- [19] Williams J K and Dawe R A 1987 *J. Colloid Interface Sci.* **117** 81
- [20] Williams J K and Dawe R A 1988 *J. Colloid Interface Sci.* **124** 691
- [21] Ioannidis M A, Chatzis I and Payatakes A C 1991 *J. Colloid Interface Sci.* **143** 22
- [22] Conrad S H, Wilson J L, Mason W R and Peplinski W J 1992 *Water Resources Res.* **28** 467
- [23] Soll W E, Celli M A and Wilson J L 1993 *Water Resources Res.* **29** 2963
- [24] Wan J, Tokunaga T K, Tsang C-F and Bodvarsson G 1996 *Water Resources Res.* **32** 1955
- [25] Lenormand R, Zarcone C and Sarr A 1983 *J. Fluid Mech.* **135** 337
- [26] Lenormand R, Touboul E and Zarcone C 1988 *J. Fluid Mech.* **189** 165
- [27] Lenormand R 1990 *J. Phys.: Condens. Matter* **2** SA79
- [28] Lenormand R and Zarcone C 1985 *Phys. Rev. Lett.* **54** 2226
- [29] Charlaix E, Hulin J-P, Leroy C and Zarcone C 1988 *J. Phys. D: Appl. Phys.* **21** 1727
- [30] Lenormand R and Zarcone C 1989 *Transport Porous Media* **4** 599
- [31] Chen J-D 1986 *J. Colloid Interface Sci.* **110** 488
- [32] Morris J P, Cheng J-T, Tran J, Lumsdaine A, Giordano N and Pyrak-Nolte L J 2001 to be published
- [33] Cheng J-T 2001 *Thesis* Purdue University, West Lafayette, IN
- [34] Nolte D D and Pyrak-Nolte L J 1991 *Phys. Rev. A* **44** 6320
- [35] Regnier F 1999 *Chromatographica Suppl. I* **49** S-56
- [36] Purcell E M 1977 *Am. J. Phys.* **45** 3
- [37] Brody J P, Yager P, Goldstein R E and Austin R H 1996 *Biophys. J.* **71** 3430
- [38] Kenis P J A, Ismagilov R F and Whitesides G M 1999 *Science* **285** 83
- [39] Kamholz A E, Weigl B H, Finlayson B A and Yager P 1999 *Anal. Chem.* **71** 5340
- [40] Ismagilov R F, Stroock A D, Kenis P J A, Whitesides G and Stone H A 2000 *Appl. Phys. Lett.* **76** 2376
- [41] Zhang W, Stone H A and Sherwood J D 1996 *J. Phys. Chem.* **100** 9462
- [42] Knight J B, Vishwanath A, Brody J P and Austin R H 1998 *Phys. Rev. Lett.* **80** 3863
- [43] Elwenspoek M, Lammerink T S J, Miyake R and Fluitman J H J 1994 *Analysis* **22** M9
- [44] Volkmarth W D and Austin R H 1992 *Nature* **358** 600
- [45] Austin R H and Volkmarth W D 1993 *Analysis* **21** 235
- [46] He B, Tait J and Regnier F 1998 *Anal. Chem.* **70** 3790
- [47] He B and Regnier F 1998 *J. Pharmacol. Biomed. Anal.* **17** 925
- [48] He B, Tan L and Regnier F 1999 *Anal. Chem.* **71** 1464
- [49] Duffy D C, Schueller O J A, Brittain S T and Whitesides G M 1999 *J. Micromech. Microeng.* **9** 211
- [50] Grossman P D and Colburn J C (ed) 1992 *Capillary Electrophoresis* (San Diego, CA: Academic)
- [51] Manz A, Miyahara Y, Miura J, Watanabe Y, Miyagi H and Sato K 1990 *Sensors Actuators B* **1** 249

- [52] Harrison D J, Manz A, Fan Z, Hüdi L and Widmer H M 1992 *Anal. Chem.* **64** 1926
- [53] Effenhauser C S, Manz A and Widmer H M 1993 *Anal. Chem.* **65** 2637
- [54] Effenhauser C S, Paulus A, Manz A and Widmer H M 1994 *Anal. Chem.* **66** 2949
- [55] Chiem N and Harrison D J 1997 *Anal. Chem.* **69** 373
- [56] Effenhauser C S, Bruin G J M, Paulus A and Ehrat M 1997 *Anal. Chem.* **69** 3451
- [57] Waters L C, Jacobson S C, Kroutchinina N, Khandurina J, Foote R S and Ramsey M J 1998 *Anal. Chem.* **70** 158
- [58] Northrup M A, Benett B, Hadley D, Landre P, Lehew S, Richards J and Sratton P 1998 *Anal. Chem.* **70** 918
- [59] Ertaş D 1998 *Phys. Rev. Lett.* **80** 1548
- [60] Duke T A and Austin R H 1998 *Phys. Rev. Lett.* **80** 1552
- [61] Chou C-F, Bakajin O, Turner S W P, Duke T A J, Chan S S, Cox E C, Craighead H G and Austin R H 1999 *Proc. Natl Acad. Sci. USA* **96** 13 762
- [62] Volkmarth W D, Duke T, Wu M C, Austin R H and Szabo A 1994 *Phys. Rev. Lett.* **72** 2117
- [63] Volkmarth W D, Duke T, Austin R H and Cox E C 1995 *Proc. Natl Acad. Sci. USA* **92** 6887
- [64] Duke T, Monnelly G, Austin R H and Cox E C 1997 *Electrophoresis* **18** 17
- [65] DeBlois R W and Bean C P 1970 *Rev. Sci. Instrum.* **41** 909
- [66] Chiu D T, Jeon N L, Huang S, Kane R S, Wargo C J, Choi I S, Ingber D E and Whitesides G M 2000 *Proc. Natl Acad. Sci. USA* **97** 2408
- [67] Stroock A D, Weck M, Chiu D T, Huck W T S, Kenis P J A, Ismagilov R F and Whitesides G M 2000 *Phys. Rev. Lett.* **84** 3314
- [68] Jeon N L, Choi I S, Xu B and Whitesides G M 1999 *Adv. Mater.* **11** 946
- [69] Decher G 1996 *Comprehensive Supramolecular Chemistry* vol 9 (Oxford: Pergamon) p 507
- [70] Hammond P T and Whitesides G M 1995 *Macromolecules* **28** 7569
- [71] Stroock A D, Weck M, Chiu D T, Huck W T S, Kenis P J A, Ismagilov R F and Whitesides G M 2001 to be published
- [72] Thompson P A and Troian S M 1997 *Nature* **389** 360
- [73] Stevens M J, Mondello M, Grest G S, Chui S T, Cochran H D and Cummings P T 1997 *J. Chem. Phys.* **106** 7303
- [74] Cieplak M, Koplik J and Banavar J R 1999 *Physica A* **274** 281
- [75] Granick S 1991 *Science* **253** 1374
- [76] Chan D Y C and Horn R G 1985 *J. Chem. Phys.* **83** 5311
- [77] Van Alsten J and Granick S 1988 *Phys. Rev. Lett.* **61** 2570
- [78] Gee M L, McGuigan P M and Israelachvili J N 1990 *J. Chem. Phys.* **93** 1895
- [79] Georges J M, Millot S, Loubet J L and Tonck A 1993 *J. Chem. Phys.* **98** 7345
- [80] Pit R, Hervet H and Léger L 1999 *Tribol. Lett.* **7** 147
- [81] Pit R, Hervet H and Léger L 2000 *Phys. Rev. Lett.* **85** 980
- [82] Yu D, Hsieh H Y and Zemel J N 1993 *Sensors Actuators A* **39** 29
- [83] Liu J and Tai Y-C 1995 *IEEE Workshop on Micro Electro Mechanical Systems* vol 8 (New York: IEEE) p 209
- [84] Harley J C, Huang Y, Bau H H and Zemel J N 1995 *J. Fluid Mech.* **284** 257
- [85] Pfahler J, Harley J and Bau H 1990 *Sensors Actuators A* **21–23** 431
- [86] Pfahler J, Harley J, Bau H and Zemel J N 1991 *Micromech. Sensors Actuators Syst.* **32** 49
- [87] Pfahler J N 1992 *PhD Thesis* University of Pennsylvania, Philadelphia, PA
- [88] Urbanek W, Zemel J N and Bau H H 1993 *J. Micromech. Microeng.* **3** 206